Population dynamics can be more important than physiological limits for determining range shifts under climate change

DAMIEN A. FORDHAM*, CAMILLE MELLIN*†, BAYDEN D. RUSSELL‡,
REŞIT H. AKÇAKAYA§, COREY J. A. BRADSHAW*¶, MATTHEW E. AIELLO-LAMMENS§,
JULIAN M. CALEY†, SEAN D. CONNELL§, STEPHEN MAYFIELD¶,
SCORESBY A. SHEPHERD¶ and BARRY W. BROOK*

*The Environment Institute, School of Earth and Environmental Sciences, The University of Adelaide, Adelaide, SA 5005, Australia, †Australian Institute of Marine Science, PMB No.3, Townsville, QLD 4810, Australia, ‡Southern Seas Ecology Laboratories, School of Earth and Environmental Sciences, The University of Adelaide, Adelaide, SA 5005, Australia, §Department of Ecology and Evolution, Stony Brook University, Stony Brook, NY 11794, USA, ¶South Australian Research and Development Institute, Henley Beach, SA 5022, Australia

Abstract

Evidence is accumulating that species' responses to climate changes are best predicted by modelling the interaction of physiological limits, biotic processes and the effects of dispersal-limitation. Using commercially harvested blacklip (*Haliotis rubra*) and greenlip abalone (*Haliotis laevigata*) as case studies, we determine the relative importance of accounting for interactions among physiology, metapopulation dynamics and exploitation in predictions of range (geographical occupancy) and abundance (spatially explicit density) under various climate change scenarios. Traditional correlative ecological niche models (ENM) predict that climate change will benefit the commercial exploitation of abalone by promoting increased abundances without any reduction in range size. However, models that account simultaneously for demographic processes and physiological responses to climate-related factors result in future (and present) estimates of area of occupancy (AOO) and abundance that differ from those generated by ENMs alone. Range expansion and population growth are unlikely for blacklip abalone because of important interactions between climate-dependent mortality and metapopulation processes; in contrast, greenlip abalone should increase in abundance despite a contraction in AOO. The strongly non-linear relationship between abalone population size and AOO has important ramifications for the use of ENM predictions that rely on metrics describing change in habitat area as proxies for extinction risk. These results show that predicting species' responses to climate change often require physiological information to understand climatic range determinants, and a metapopulation model that can make full use of this data to more realistically account for processes such as local extirpation, demographic rescue, source-sink dynamics and dispersal-limitation.

Keywords: abalone, demographic processes, ecological niche model, extinction risk, marine biodiversity conservation, marine species distribution model, mechanistic model, metapopulation dynamics, population viability analysis, source-sink dynamics

Introduction

Human-driven global climate disruption is affecting the demography, geographical distributions and phenologies of many marine species (Clark *et al.*, 2003; Edwards & Richardson, 2004; Perry *et al.*, 2005; Dulvy *et al.*, 2008). These impacts stem from biophysical responses to ocean temperature change and other related climate-driven oceanographic phenomena such as hypoxia and acidification (Pörtner, 2010). Additional future warming and acidification are expected to continue to alter marine ecosystems rapidly (Harley *et al.*, 2006), as well as modify the economic and social systems that depend on them (Sumaila *et al.*, 2011).

Past and predicted changes in the distributions and abundances of marine and terrestrial species are commonly estimated using correlative ecological niche models (ENMs) (also referred to as 'species distribution models' or 'bioclimatic envelope models') (Franklin, 2009; Peterson *et al.*, 2011; Araújo & Peterson, 2012). However, mechanistic modelling approaches that account explicitly for species-specific physiological traits are being applied more frequently to questions of how species' distributions will respond to climate change (Crozier & Dwyer, 2006; Kearney *et al.*, 2008;

Cheung *et al.*, 2011). Linking functional traits with environmental conditions should result in more robust predictions of range shifts in situations where human-mediated environmental change has already altered a species' observed range, or where distribution data inadequately represent important environmental gradients due to historical effects (i.e. through localized depletion from harvesting) (Buckley *et al.*, 2010). These more robust predictions arise because biophysical models more directly capture a species' fundamental niche by incorporating explicit relationships between environmental conditions and organismal performance, estimated independently of the species' current distribution (Kearney & Porter, 2009). In contrast, ENMs rely on statistical correlation to estimate a species' realized niche using phenomenological methods that relate current distributions to environmental conditions (Peterson *et al.*, 2011). This approach implicitly assumes that species occupy their entire range of habitable environmental conditions (Araújo & Peterson, 2012); however, this assumption is rarely true, often for historical reasons (Monahan, 2009). Although this problem can be addressed directly in ENMs through a better understanding of how abiotic conditions and dispersal potential have influenced a species geographical distribution over time (Nogués-Bravo, 2009; Barve *et al.*, 2011), this approach is rarely used.

Biophysical models should, in theory, be more useful than ENMs for predicting the dynamics of range limits through time, because the assumption that available occurrence data represent the species' entire range is relaxed (Kearney & Porter, 2009). However, the extent to which biophysical models perform better than ENMs is species- and ecosystem specific (Buckley, 2008; Kearney *et al.*, 2010). Biophysical models are preferable to ENMs if a species' range and abundance are constrained by a particular physiological response, or if its distribution is not in equilibrium with current climate conditions (Buckley *et al.*, 2010). Nevertheless, ENMs can still be useful, especially when calibrated using data from multiple time periods (Maiorano *et al.*, 2013). They are simpler to parameterize than biophysical models, and can be readily applied in any situation where location and climate data are available (Dormann *et al.*, 2012). Moreover, ENM performance improves with the inclusion of physiological information (Buckley *et al.*, 2011). These 'biophysical-ENMs' can be developed using physiological approaches to (i) select biologically relevant ENM predictors (Austin, 2007; Austin & Van Niel, 2011); (ii) constrain ENM pseudo-absence selection (Elith *et al.*, 2010); and (iii) identify a species' potential distribution that is more closely aligned with its fundamental niche (Monahan, 2009).

However, to account properly for important biotic processes such as source-sink and density-feedback dynamics, and interacting effects of habitat fragmentation and demographic stochasticity in species distributions, a demographic model is needed (Fordham *et al.*, 2012a). Methods that link ENMs with biophysical and metapopulation dynamics might therefore better estimate range shifts under climate change by accounting for additional biological and landscape processes (Keith *et al.*, 2008; Anderson *et al.*, 2009). Linking life-history traits and spatial data also permits population density to vary as a function of climate gradients (including through biophysical responses), habitat modification, exploitation and species interactions, which in turn modify survival and fertility (Fordham *et al.*, 2013a).

Potential physical changes in body size and range shifts in marine fishes in response to climate change have recently been predicted using a coupled biophysical-population model accounting for physiological responses to hypoxia, preferences and tolerances to environmental conditions, dispersal and population dynamics (Cheung *et al.*, 2012). While sophisticated, this model did not account for source-sink dynamics (partly because it was built at a global scale), and so potentially overlooked important dispersal and metapopulation processes. The explicit incorporation of metapopulation processes, modified dynamically by exploitation and climate change, could have improved the model's predictive performance. Here, we advance the modelling approach of Cheung *et al.* (2012) by linking ENMs with stochastic demographic models that account for biophysical processes and fine-scale metapopulation dynamics. We then investigate interacting effects of climate change and other anthropogenic stressors, such as commercial harvest, on the population size and range dynamics of two commercially exploited molluscs (blacklip abalone *Haliotis rubra* and greenlip abalone *Haliotis laevigata*) inhabiting coastal reefs of South Australia.

We previously used relatively simple ENMs to predict that climate change might benefit the Australian abalone industry, which is worth >$200 million annually (Russell *et al.*, 2012). Given the constraints of traditional ENMs, we were forced by the model structure to assume that exploitation and dispersal limitation had not influenced the range of habitable conditions occupied by *H. rubra* and *H. laevigata* today. Here, we can relax these assumptions and test this hypothesis explicitly using more sophisticated approaches appraising model predictions with respect to interactions between physiological responses, metapopulation dynamics and exploitation under various climate change scenarios. Specifically, we compare the influence of three classes of species distribution models (ENMs, biophysical-ENMs and

niche-population models) on current occupancy and future predictions of abundance for two abalone species under contrasting climate futures, generated using multiple atmosphere-ocean general circulation models and greenhouse gas emission scenarios. We interrogate alternative forecasting methods to address whether predictions of species' responses to climate change require physiological information to predict the relative importance and magnitude of climatic range determinants, and a metapopulation model that accounts for biotic processes and dispersal-limitation effects.

Materials and methods

Climate data

To understand the relationship between present-day abalone abundance and sea-surface temperatures (SST), we generated high-resolution gridded mean monthly SSTs (0.01° resolution) for August and March (coolest and warmest months respectively) for a 20-year baseline period 1985–2004 around South Australia (Mellin *et al.*, 2012). To explore future climatic trends relevant to abalone population abundance, we produced annual climate forecasts for August and March SST according to two global emission scenarios: (i) a no-climate-policy reference scenario (MiniCAM Ref) that models a CO_2 concentration of ca. 750 ppm in 2100, and (ii) a corresponding policy scenario (MiniCAM, Lev1) designed to stabilize at an equivalent CO_2 concentration of 450 ppm (Clarke *et al.*, 2007; Wigley *et al.*, 2009). We used MAGICC/SCENGEN 5.3 (Fordham *et al.*, 2012c) to generate an annual time series of future climate anomalies (2000–2100) based on an evenly weighted ensemble of seven atmosphere-ocean general circulation models (GCM) (see Fordham *et al.*, 2013b for a description of the seven GCMs and why they were chosen), and individually for two contrasting GCMs – the parallel climate model (PCM; Washington *et al.*, 2000) and the Community Climate System Model, version 3.0 (CCSM-3; Collins *et al.*, 2006) (see Appendix S1 for details). Collectively, these models provide a suite of representative climate futures, with the PCM predicting the lowest increase in summer (March) SST and the greatest increase in winter (August) SST, and the seven-model average providing intermediate forecasts between those given by PCM and CCSM-3 for March SST (Fig. S1). We downscaled SST forecasts to a 0.01° resolution using the 'change factor' empirical method, where the MAGICC/SCENGEN low-resolution climate anomaly (change from an observation period centred on 1990) is added directly to a high-resolution baseline of observed SST, centred on or around 1990 (Russell *et al.*, 2012). We applied bilinear interpolation of the GCM data (2.5° resolution) to a finer resolution (0.5°) to reduce discontinuities in the perturbed climate at the GCM grid-box boundaries (Fordham *et al.*, 2011).

Abundance and environmental data

Spatial abundance data for *H. rubra* and *H. laevigata* were based on repeated annual SCUBA surveys that specifically targeted commercially harvested reefs (1980–2009), and semi-annual surveys (2004–2009) of randomly chosen reefs across the entire state of South Australia (Mellin *et al.*, 2012). Probabilities of occurrence for inshore reefs in South Australia were derived using bathymetric data and artificial neural networks at a 250-m resolution (Watts *et al.*, 2011). We obtained mean depth from a ca. 250-m resolution multi-beam bathymetry provided by Geoscience Australia (Webster & Petkovic 2005). Data were aggregated to a 0.01° resolution (Mellin *et al.*, 2012). We collated the geographical coordinates of boat ramps used by both recreational and commercial abalone fishing vessels and calculated the Euclidean distance to the nearest boat ramp for every grid cell in ArcGIS 9.2. (Environmental Systems Research Institute, Redlands, CA, USA) We sourced commercial catch data for abalone from the SARDI Aquatic Sciences. A more detailed description of abalone survey methods and environmental data is provided by Mellin *et al.*, 2012.

Ecological niche model

We modelled spatially explicit abundance patterns of *H. rubra* and *H. laevigata* separately for each species across their ranges (north of latitude 39.5°S) using an ensemble ecological niche-modelling approach that combined likelihood-based generalized linear models and boosted regression trees. For each modelling technique, we applied a two-step procedure to predict (at ca. 1 × 1-km grid cell resolution): (i) the current probability of presence, followed by (ii) current abundance conditional on presence (Mellin *et al.*, 2012). Previous work showed that the best primary predictors of abundance were mean coolest monthly (August) SST and, to a lesser extent, its SD. A positive linear correlation between August SST and *H. rubra* abundance explained 34% of model structural deviance; a positive quadratic relationship for *H. laevigata* explained 17% of deviance (Mellin *et al.*, 2012). Harvest intensity, water depth and distance from the nearest boat launching point were also important predictors. Collectively, all predictors accounted for up to 55% and 45% of deviance explained in the abundance of *H. rubra* and *H. laevigata* respectively (Mellin *et al.*, 2012). ENMs were validated using an independent dataset (for *H. rubra* only because of restricted data availability), as well as standard 10-fold cross-validation (see Mellin *et al.*, 2012 for the validation results). We used annual climate forecasts of August SST (2000–2100) as an input in the ENM abundance models to generate a 100-year time series of spatial abundance predictions for *H. rubra* and *H. laevigata* (see Appendix S1 for further details). All other predictors were modelled as static variables (Stanton *et al.*, 2012). Because *H. rubra* and *H. laevigata* are restricted to rocky reef habitat (McShane & Smith, 1991; Shepherd, 1998), predicted abundance estimates for each species accounted for the proportion of each grid cell expected to include rocky reef habitat (based on Watts *et al.*, 2011).

Coupled niche-population model

We built coupled niche-population models (Fordham *et al.*, 2013a) for *H. rubra* and *H. laevigata* in RAMAS GIS v5

(Akçakaya & Root, 2005). We divided the study region (as described by Russell *et al.*, 2012; and shown in Fig. 1) into $0.01 \times 0.01°$ grid cells. We based the spatial structure of the metapopulation (the location and connectedness of occupied rocky reefs) on spatial predictions of abalone carrying capacities for individual reefs generated using ENM predictions and adjusted to account for an under-representation of juveniles (see Appendix S1 for details).

We developed a pre-breeding, stage-structured matrix model (Akçakaya & Root, 2005). Matrix elements governed transitions among seven length classes (size classes are provided in Bardos *et al.*, 2006), derived for a time step of 1 year from growth, fertility and mortality data for abalone populations in Australia (Appendix S1). Fertility and allometric growth rates were the same as those used by Bardos *et al.* (2006) for a fast-growing abalone population. We set annual survival in the largest size class (>118 mm) at 0.72 based on locally derived estimates for non-harvested populations of *H. laevigata* (Shepherd, 1990). We modified survival rates for size classes used by Bardos *et al.* (2006) proportionally so that the upper limit on annual survival was 0.72 (Appendix S1).

Abalone recruitment and abundance are highly variable, even in the absence of fishing (Mayfield *et al.*, 2012), probably due to variability in SST (Shepherd & Brown, 1993). We initially modelled year-to-year variability in vital rates for *H. laevigata* and *H. rubra* using a coefficient of variation (CV) of 0.282 for survival (animals >3 years) and 0.85 for fertility (see Appendix S1 for details). We then adjusted the vital rate variability so that annual fluctuations in the model's output of total metapopulation size matched the observed variability in *H. laevigata* abundance (based on Shepherd, 1990), computed as the CV of $\log\left(\frac{N_t + 1}{N_t}\right)$ (where N_t is the population size a time t) (Anderson *et al.*, 2009). The revised CV parameters were 0.20 and 0.78 for survival and fertility respectively. We modelled density feedback using a Ricker (logistic) equation, modelling a process of deteriorating conditions as density of animals aged >12 months increases. Survival rates varied proportionally when subpopulation abundance increased above half of carrying capacity (see below). We simulated an Allee effect, whereby fertilization success decreased with female adult density below 0.1 individuals m^{-2} (Babcock & Keesing, 1999). We estimated maximum rate of intrinsic population growth (R_{max}, exp [r_m]) using two independent long-term sur-
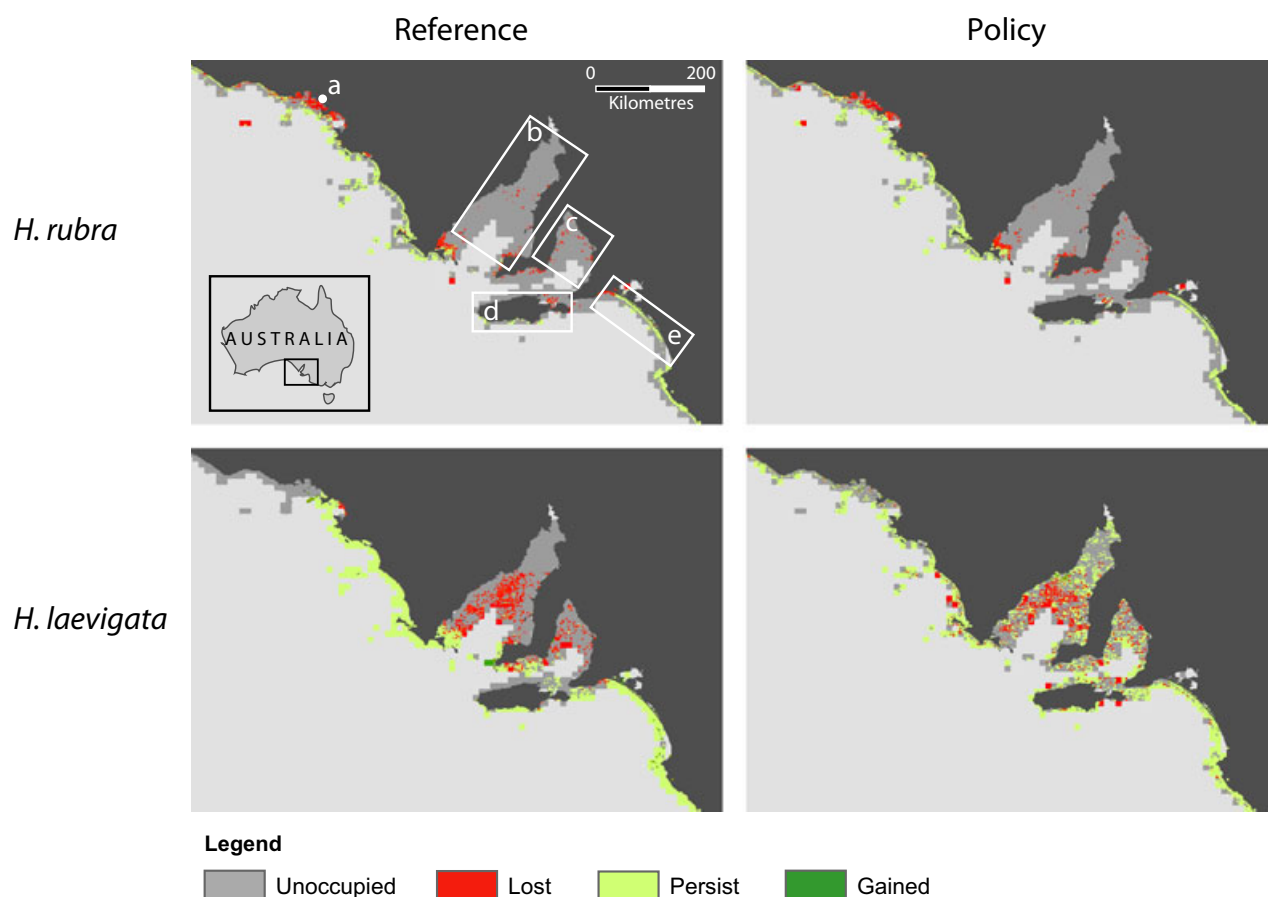

Fig. 1 Forecast change in grid cell occupancy between 2015 and 2090 according to niche-population models under *reference* and *policy* emission scenarios. The direction of change for each cell is based on agreement between at least two of the three general circulation model approaches (7-model ensemble, CCSM-3 and PCM). Shown are (a) the town of Ceduna, (b) Spencer Gulf, (c) Gulf St Vincent, (d) Kangaroo Island and (e) Coorong.

veys (each >13 years) of *H. laevigata* abundance (Shepherd, 1990; Shepherd & Partington, 1995). By fitting a linear relationship between realized r and population size (Fordham *et al.*, 2012b), we estimated R_{max} at 1.82. The estimates for equilibrium carrying capacity (K, when $r = 0$) were reef-specific and dynamic over time, being dependent on the sum of abundances for all reef grid cells as generated by the ENMs. The ENM predictions probably underestimated juvenile abalone abundances because they are cryptic and difficult to detect using underwater surveys (Shepherd, 1990). To account for the influence of survey bias on estimates of K, we multiplied grid cell abundance by the ratio of juvenile to adults expected under a stable age distribution.

Temperatures >17 °C for *H. rubra*, and 18.3 °C for *H. laevigata*, affect juvenile recruitment and growth negatively (Shepherd & Breen, 1992; Harris *et al.*, 2005). Temperatures >21 °C (*H. rubra*) and 22.5 °C (*H. laevigata*) cause a detrimental behavioural response in adults, inhibiting feeding and growth (Gilroy & Edwards, 1998). The critical thermal maxima (LD_{50} i.e. temperature at which 50% of animals die) is ca. 27 °C, but temperature-related deaths can occur even at 24.5 °C for some individuals (Gilroy & Edwards, 1998). We modelled fertility and survival conditioned by SST in the hottest month of the year (March). We used a 1 °C buffer to account for the mean difference between sea surface and seabed temperatures (Fordham *et al.*, 2013b). For *H. rubra* and *H. laevigata,* respectively, recruitment of 12-month-old animals declined linearly between 18 and 22 °C and 19.3–23.5 °C (with no recruitment at temperatures ≥22 °C or 23.5 °C). Relative survival declined linearly between 25 and 30 °C for both species.

We modelled populations as primarily self-recruiting, with little larval exchange at distances up to 20 km (Miller *et al.*, 2009). We constrained dispersal to the 0- to 12-month-old size class (McShane *et al.*, 1988) and modelled ca. 90% of animals moving less than 1 km (i.e. staying within a single grid cell) and 1% moving 10 km. We used regional variation in August year-to-year SST to approximate the spatial correlation in environmental variability. We set environmental variability to be correlated between populations, with stronger correlations for neighbouring populations. We calculated pairwise correlations as $P = \exp(D/b)$ where D is the distance between centroids of habitat patches and $b = 90$ (Akçakaya & Root, 2005). Similar approaches have been used to model environmental variability in terrestrial systems (Anderson *et al.*, 2009; Fordham *et al.*, 2012a).

Abalone harvesters tend to target large aggregations of older animals with shell lengths >125–145 mm (slightly larger than the largest size class in our model), depending on the species and fishing zone, changing fishing location when catch rates and associated densities decline (McShane & Smith, 1989), among other factors. For each harvestable reef (i.e. reef in a harvest zone and of sufficient size, see below), annual catch mortality of animals >118 mm varied from 20 to 30% every 1–2 years for *H. rubra*; and 20–40% every 1–3 years for *H. laevigata*. We set these harvest rates based on expert advice, taking into account long-term fishing records (Mayfield *et al.*, 2011). We modelled the minimum size of harvested animals as spatially invariant and constant across species. Since reliable age-based growth data for wild abalone >118 mm are limited,

we set minimum harvest size at 118 mm, not the minimum legal length enforced by government regulation. Because fishing mortality and harvest frequency varies from year-to-year at each reef, we randomly varied these parameters for each reef across model iterations. To simulate important population refugia (Shepherd & Brown, 1993), arising through a commercial preference to harvest from larger more profitable reefs, we set the minimum reef size that could support commercial harvests at 0.0146 km^2 so that 5% of reefs within the harvest region were not large enough to be harvested. On the basis of commercial harvest practices in South Australia, we constrained harvests to years (and sites) when large adult (>118 mm) densities were >0.2 and 0.1 m^{-2} for *H. rubra* and *H. laevigata* respectively. To avoid using a static threshold, we modelled a steep linear increase in harvest from 0.2 to 0.25 individuals m^{-2} for *H. rubra* and 0.1–0.15 individuals m^{-2} for *H. laevigata*.

We predicted area of occupancy (AOO) at 1-km grid cell resolution (see below), abundance and harvest for each species for each year between 2000 and 2100 using climate forecasts from two greenhouse-gas-emission scenarios (MiniCAM Ref and Lev1) according to an ensemble of seven GCMs (7-model) and two individual GCMs (CCSM-3 and PCM). In these scenarios, species' spatial abundance patterns were driven by demographic and biophysical processes, commercial harvesting, climate change and their interactions. We based all simulations on 1000 stochastic replicates of RAMAS Metapop (Akçakaya & Root, 2005) run over 101 years (2000–2100). We discarded the first 15 years of the simulation as a 'burn in' to ensure that metrics of change were calculated from a stable age distribution and equilibrium initial reef abundance (Fordham *et al.*, 2012b). Thus, model results summarize projections for the period 2015–2100.

We assessed niche-population model performance using a 40-year time series of catch data (Mayfield *et al.*, 2012). Models for both *H. rubra* and *H. laevigata* approximated species-specific catches for the South Australian fishery. Observed annual catches are ca. 480 t for *H. rubra* and 390 t for *H. laevigata*. Mean predicted annual catches, based on model simulations without climate change, were 484 t for *H. rubra*, with a minimum annual harvest >267 t. For *H. laevigata*, they were 460 t with a minimum catch >315 t, making modelled catches about 15% higher than observed rates. This is not problematic because catch tends to underestimate annual harvests since catch estimates do not account for illegal and recreational catches (Plagányi *et al.*, 2011).

Biophysical ecological niche model

We restricted forecast abundance from ENMs to grid cells with SST below species-specific thermal-tolerance levels (see above). Specifically, ENM predictions of K were set to zero above thermal thresholds where the survival, and hence recruitment, of abalone aged between 0 and 12 months is expected to decrease by more than 50% (corresponding to 20.05 °C for *H. rubra* or 21.4 °C for *H. laevigata*) or by more than 80% (corresponding to 21.22 °C for *H. rubra* or 22.65 °C for *H. laevigata*).

Model comparisons

We compared forecasts of relative change in abundance and AOO between 2015 and 2100 for three different modelling approaches: (i) ENMs with no biophysical constraints; (ii) biophysical-ENMs, where ENM predictions of K were set to zero above thermal-tolerances for recruitment; and (iii) niche-population models that explicitly model biophysical and demographic responses to climate change and commercial harvesting. We calculated change in AOO as the difference between the number of grid cells (0.01° resolution cells encompassing subtidal rock habitats) gained by the species [sites where abundance in a grid cell exceeded the density threshold (see below) in 2100, but fell below the threshold in 2015] and the number of grid cells lost (sites where the species was forecast to be absent in 2100, but present in 2015) relative to the total number occupied in 2015. We applied a density threshold of 500 individuals cell^{-1} (females >12 month old) to spatial density maps (2015–2100), being equivalent to approximately 3 large females km^{-2} (>118 mm shell length). Thus, we ignored low-density populations that are biologically unviable (Shepherd & Brown, 1993) in estimates of range shifts (Fordham *et al.*, 2012a).

We compared predictions of present-day occurrence patterns using 10-fold cross-validation for each species. We randomly partitioned abundance data into 10 equal sized subsamples and used nine subsamples to generate both an ENM and a niche-population model, validating these models against the remaining subsample. We repeated this process 10 times, so that each subsample was used only once for validation. We ran niche-population models for 1000 simulations over 15 years. We calculated Cohen's kappa statistic (κ) (Cohen, 1960) for each model based on a confusion matrix, expressing matches and mismatches of observed and predicted occurrences in the validation data set. We computed this matrix after using receiver operating characteristic curves to select a threshold for converting continuous abundance predictions into predictions of presence-absence (Liu *et al.*, 2005). We used root mean-squared error (RMSE) to compare the predictive errors for abundance.

Sensitivity analysis and model uncertainty

We estimated the influence of spatial and non-spatial parameters on niche-population model predictions of abundance. To ensure sampled values covered the entire parameter space, we used Latin hypercube sampling (Iman *et al.*, 1981) with 50 sampling dimensions, drawing values for each parameter randomly from within 50 evenly sized partitions across realistic ranges of the following parameters: R_{max} (±10%), dispersal (±10%), variability in vital rates (±10%), carrying capacity (±20%) and harvest off-take (±20%) (see Appendix S1 for details). To see whether results from ENMs and biophysical-ENMs differ substantially from niche-population models, we plotted the 5th and 95th percentiles of predicted change in population size using results from these sensitivity analyses.

Results

Model comparisons

Niche-population models and biophysical-ENMs predicted that *H. rubra* and *H. laevigata* will experience large contractions in AOO by 2100 for nearly all emission scenarios and climate modelling approaches (Figs 1–3 and S2–S5). However, niche-population models tended to predict smaller losses of AOO under the reference emission scenario compared to biophysical-ENMs (Table 1). ENMs predicted marginal changes in AOO for *H. rubra* and *H. laevigata*, regardless of emission scenario or climate modelling approach (Table 1).

Projected spatial patterns of abundance were highly dependent on modelling technique (Figs 2 and 3). Notably, sites where abundance decreased, but populations were not extirpated, were more frequent for niche-population models compared to other techniques. Niche-population models forecast decreases in population size for *H. rubra* between 2015 and 2100 under both emission scenarios for 7-model and CCSM-3 (Figs 4 and S6). Conversely, *H. laevigata* population size was predicted to increase under the reference scenario between 2015 and 2100 (Figs 4 and S6) despite a forecast contraction in AOO (Table 1). Biophysical-ENMs predicted a negative trend in *H. rubra* population abundance, and mostly little change in *H. laevigata* population abundance, under the reference scenario for 7-model and CCSM-3 (Figs 4 and S6). In contrast, ENMs predicted large increases in population abundance under a reference emission scenario for *H. rubra* and *H. laevigata*.

Cross-validation measures of the kappa (κ) statistic showed that both ENMs and niche-population models performed reasonably well in predicting presence-absence data for *H. rubra* ($\kappa = 0.57$ and 0.48 respectively) and *H. laevigata* ($\kappa = 0.53$ and 0.41 respectively) today. The abundance prediction error for ENMs and niche-population models were also similar for *H. rubra* (RMSE = 0.267 and 0.265) and *H. laevigata* (RMSE = 0.043 and 0.064). However, niche-population models were better at predicting presence-absence data at reefs that were not used to build or validate the models (i.e. more 'distant' out-of-sample data). For example, they correctly predicted the absence of abalone (both for the present-day and for 2015) on the northern shore of Kangaroo Island, the upper Spencer Gulf, and the southern section of Gulf St Vincent (see unoccupied cells in locations *a–d* on Fig. 1). Biophysical-ENMs, with a 50% recruitment thermal threshold applied, correctly predicted the absence of abalone in the upper Spencer Gulf and areas of Gulf St Vincent, and for *H. laevigata* west of Ceduna.

Table 1 Percent change in abundance and AOO for *Haliotis rubra* and *Haliotis laevigata* between 2015 and 2100.

Modelling approach	Climate	GCM	H. rubra		H. laevigata	
			Abund.	Range	Abund.	Range
NPM	Reference	7mod	−62	−44	47	−26
		CCSM	−63	−59	7	−36
		PCM	607	−4	170	21
	Policy	7mod	−33	−36	−16	−22
		CCSM	−34	−31	18	−19
		PCM	15	−2	−3	−20
ENM	Reference	7mod	120	4	78	5
		CCSM	147	4	82	5
		PCM	740	6	135	5
	Policy	7mod	15	1	12	1
		CCSM	44	2	31	2
		PCM	17	1	12	1
Bio-ENM 80%	Reference	7mod	5	−60	−2	−44
		CCSM	−76	−81	−3	−63
		PCM	376	−48	102	−20
	Policy	7mod	4	−21	9	−7
		CCSM	24	−24	18	−20
		PCM	10	−15	4	−19
Bio-ENM 50%	Reference	7mod	−80	−83	−1	−58
		CCSM	−77	−82	−73	−76
		PCM	161	−61	56	−47
	Policy	7mod	−26	−38	2	−21
		CCSM	−23	−45	16	−24
		PCM	−19	−30	−15	−27

Change in abundance (Abund.) and area of occupancy (AOO) is calculated for two emission scenarios (*reference* and *policy*), three general circulation model (GCM) approaches (7-model, CCSM and PCM) and three modelling techniques: (i) coupled niche-population model (NPM); (ii) ecological niche model (ENM); and (iii) biophysical-ENM (Bio-ENM) with an upper critical thermal threshold above which the survival of 0–12 months individuals is expected to decrease by more than 50% or 80%. Change in AOO is the difference between the number of sites (ca. 1 × 1 km latitude/longitude cells) gained by the species and the number of sites lost relative to the total number of sites occupied in 2015. See Methods for details.

Commercial catch

Catches (based on historic and present-day catches, all else being equal) of *H. rubra* are modelled to decline between 2015 and 2100 under both emission scenarios according to the 7-model (−68% and −45% respectively) and CCSM-3 (−67% and −51%), but not PCM (+716% and +19% respectively) (Fig. S7). Harvest rates of *H. laevigata* are predicted to remain stable for all emission scenarios and climate modelling techniques, except the PCM reference scenario (+320%; Fig. S7).

Sensitivity analysis and model uncertainty

Niche-population model estimates of final population size (log N) were most sensitive to assumptions regarding the carrying capacity of individual reefs (Table 2). Estimates of final population size for *H. rubra* were also strongly influenced by estimates of R_{max}. Simple ENM

predictions of relative change in abundance for *H. rubra* exceeded the upper bound of uncertainty of the niche-population model under a 7-model ensemble reference scenario (Fig. 5). However, the ENM predictions for *H. laevigata* were not notably different from the niche-population model, at least for this ensemble reference scenario, once uncertainty was taken into account.

Discussion

Previous studies have compared correlative and biophysical predictions of current and future range size for a variety of terrestrial species (Buckley, 2008; Buckley *et al.*, 2010, 2011; Kearney *et al.*, 2010). However, no one has previously contrasted explicitly the performance of models that account simultaneously for meta-population dynamics, demographic stochasticity and biophysical processes, either in marine or terrestrial environments. In taking such an approach, we showed
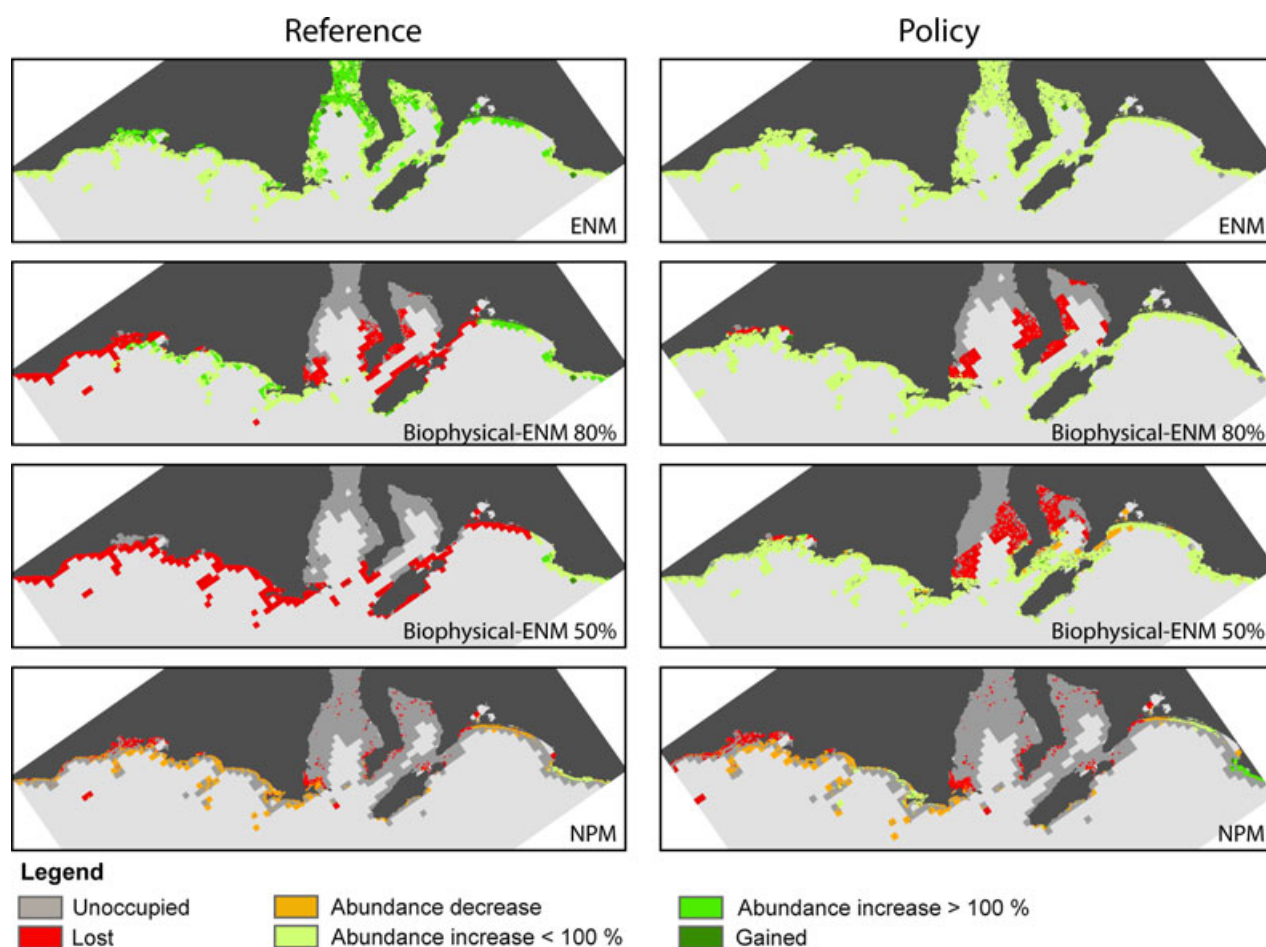
Fig. 2 Forecast change in spatial abundance between 2015 and 2100 for *Haliotis rubra* according to a regionally skilful multi general circulation model averaged forecast, two emissions scenarios (Reference and Policy) and three modelling techniques: (i) ecological niche model (ENM); (ii) biophysical-ENM with an upper critical thermal threshold above which the survival of individuals 0–12 months of age is expected to decrease by more than 50% or 80% (corresponding to 20.05 and 21.22 °C); and (iii) coupled niche-population model (NPM).

that accounting for demographic processes and physiological responses to climate-related factors can improve predictions of occupancy and abundance for two commercially exploited molluscs inhabiting coastal reefs of South Australia. We also demonstrated that ENM forecasts of population growth and expansion of South Australian abalone stocks are unlikely to occur, at least for *H. rubra*, under a more ecologically realistic framing because of important interactions between climate-dependent mortality and metapopulation processes. In short, incorporating physiological information into ENMs without simultaneously considering demographic processes can provide reliable estimates of the direction, but not necessarily the magnitude, of future changes of a species' AOO and abundance.

Earlier work on these species using only ENMs (Russell *et al.*, 2012) suggested that the Australian abalone industry could potentially benefit from climate change,

driven by warmer August SST. The favourable conditions arise largely because gonad development increases linearly with temperature up to 18 °C (Grubert & Ritar, 2004b), leading to a greater reproductive output and development rate of larvae (Grubert & Ritar, 2004a), thereby promoting earlier settlement and increased juvenile survival. However, SST in the summer months is forecast to increase at a comparable or greater rate than winter SST (Fig. S1), exceeding thermal thresholds, and thereby reducing recruitment and survival (Shepherd & Breen, 1992; Gilroy & Edwards, 1998; Harris *et al.*, 2005). Using biophysical information to modify ENM predictions (Monahan, 2009), or by modelling fertility and survival mechanistically using niche-population models with biophysical properties, we predict that climate change is more likely to reduce abalone ranges and abundances, rather than increase them, as is forecast by the simple ENMs. This
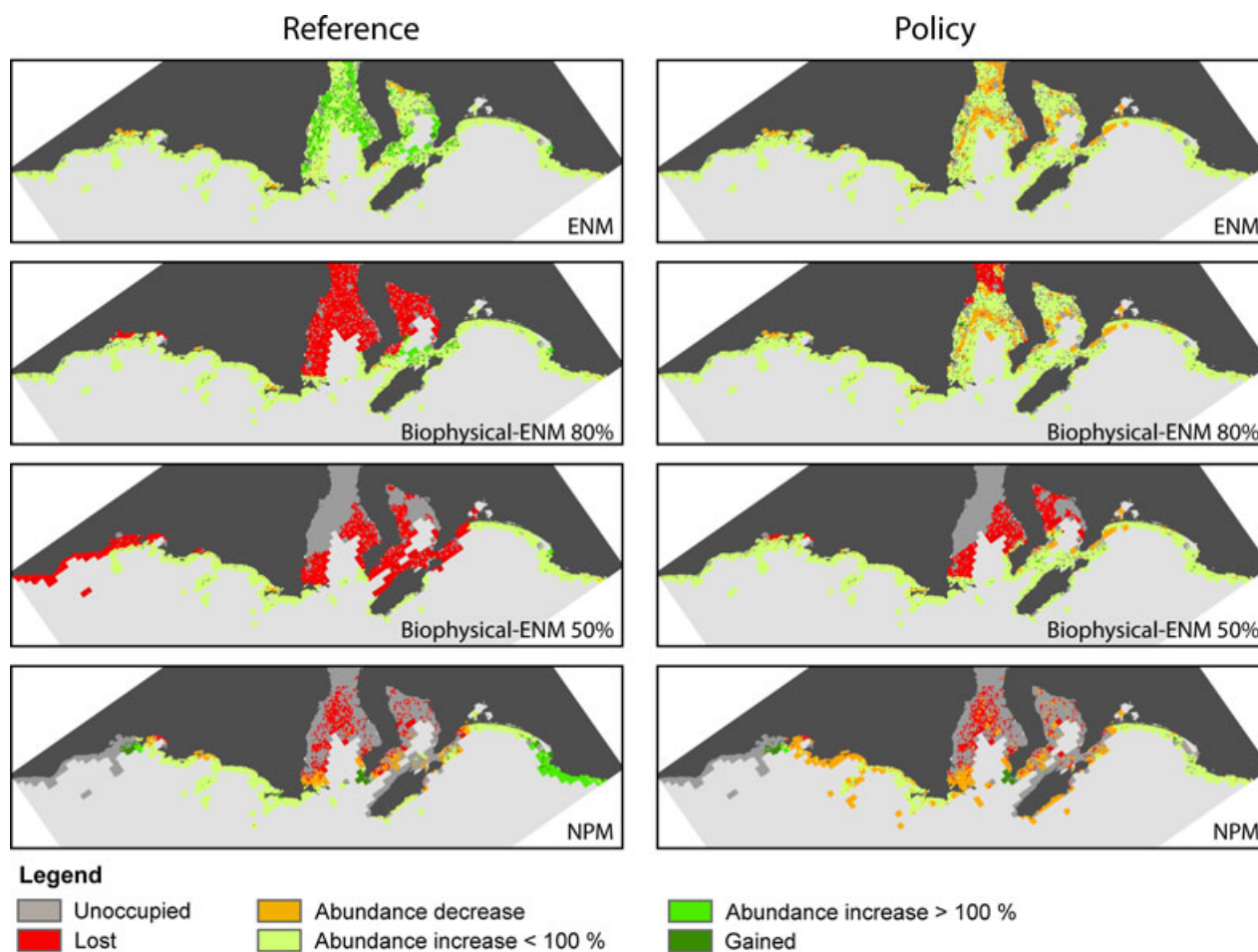
Reference Policy

Legend

Unoccupied		Abundance decrease		Abundance increase > 100 %
Lost		Abundance increase < 100 %		Gained

Fig. 3 Forecast change in spatial abundance between 2015 and 2100 for *Haliotis laevigata*. All scenarios are otherwise identical to Fig. 2 with the exception that critical thermal thresholds were 21.4 and 22.65 °C for the 50% and 80% biophysical- ENMs respectively.

discrepancy in predictions arises in part because ENMs use data in such a way as to give little consideration of the area that has been accessible to the species over time (Nogués-Bravo, 2009; Barve *et al.*, 2011), meaning that they probably did not appropriately capture the species' potential distribution.

Biophysical-ENMs for *H. rubra* predict a large reduction in AOO and declines in total population size. Declines are forecast not to occur at a proportionally constant rate, which has important ramifications for the use of habitat area-change metrics as proxies for extinction risk (see below). Niche-population models that included metapopulation dynamics and demographic processes, as well as physiological responses to thermal gradients, also predicted a non-proportional reduction in AOO and total population size. However, here the extent of change tended to be lower for niche-population models than for biophysical-ENMs, at least for AOO under the reference greenhouse gas emission

scenario. This is probably because niche-population models simulated directly the effects of population refugia and source-sink dynamics (Hanski, 1999), which can play important roles in maintaining population stability for abalone (Shepherd & Brown, 1993) and other marine organisms (Watson *et al.*, 2011). Additionally, we parameterized niche-population models using fertility responses to a gradient of March SSTs, rather than assuming an upper critical thermal threshold, resulting in gradual (and arguably more biologically realistic) declines rather than abrupt state shifts in local population densities.

Niche-population models forecast total population increases despite a contraction in AOO for *H. laevigata* under the reference greenhouse gas emission scenario, suggesting that environmental conditions on some rocky reefs will improve under pronounced climate change, and that dispersal and metapopulation dynamics can sustain recruitment to currently uninhabitable
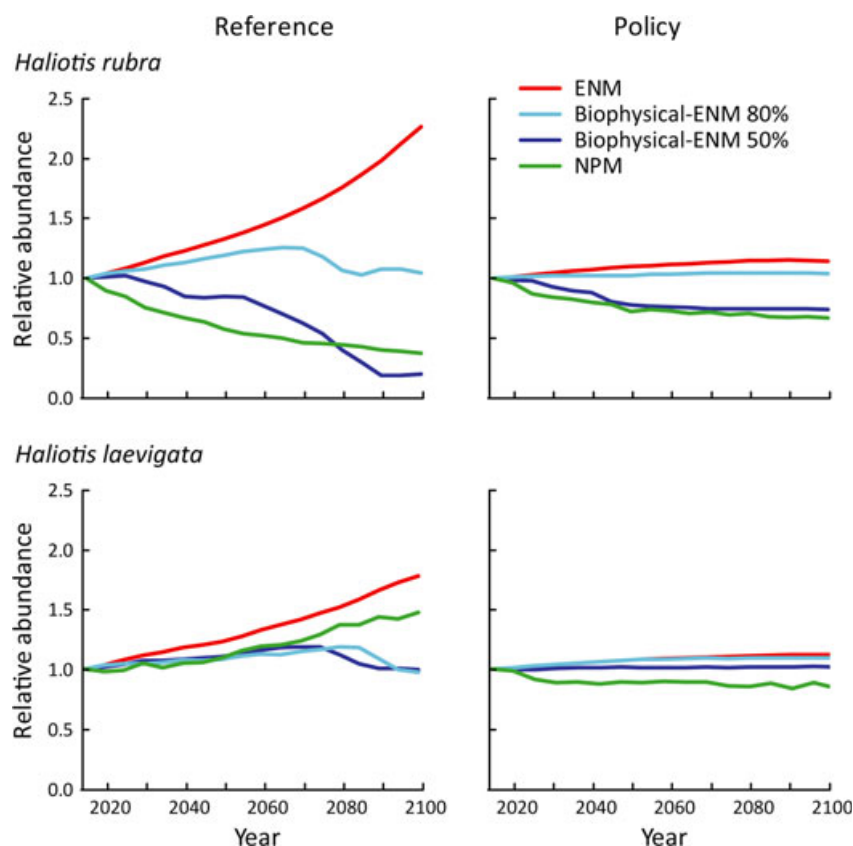
Fig. 4 Forecast change in abundance (relative to abundance in 2015) for *Haliotis rubra* and *Haliotis laevigata* (according to three model-ling approaches: (i) ecological niche model (ENM); (ii) biophysical-ENM with an upper critical thermal threshold above which the sur-vival of individuals of 0–12 months of age is expected to decrease by more than 50% or 80%; and (iii) coupled niche-population model (NPM). Differences between modelling approaches are shown for a regionally skilful multi general circulation model averaged forecast (7-mod) and two greenhouse gas emissions scenarios (*reference* or *policy*). See Methods for further details.

Table 2 Results of the Latin-hypercube-sampling sensitivity analysis for mean population size in 2100 under a reference emission scenario, based on a multi general circulation model averaged forecast

Species	Dependent variable	SRC	Coeff	Lower CI	Upper CI
Haliotis rubra	K	0.477	0.996	0.983	1.013
	R_{max}	0.405	1.943	1.924	1.971
	Var	0.067	−0.271	−0.291	−0.258
	Harv	0.039	−0.089	−0.102	−0.078
	Disp	0.011	0.046	0.026	0.062
Haliotis laevigata	K	0.734	1.082	1.073	1.090
	R_{max}	0.107	0.324	0.296	0.348
	Harv	0.091	−0.006	−0.020	0.002
	Disp	0.064	−0.267	−0.291	−0.242
	Var	0.004	0.195	0.177	0.222

Standardized regression coefficients (SRC), actual model coefficients (Coeff) and their upper and lower confidence intervals (CI) (0.025 and 0.975 bootstrap percentiles) for mean population size (log transformed) in 2100 according to the saturated general linear model, with the dependent variables: carrying capacity (K), maximum annual finite rate of population increase (R_{max}), variability in vital rates (Var), mean dispersal distance (Disp) and harvest off-take (Harv).

or suboptimal habitats that are forecast to become more suitable in the future. These observations have impor-tant consequences for ENMs that infer extinction risk

from projected changes in geographical extent, because of their underlying assumption of a linear relationship between abundance and range area (Akçakaya *et al.*,
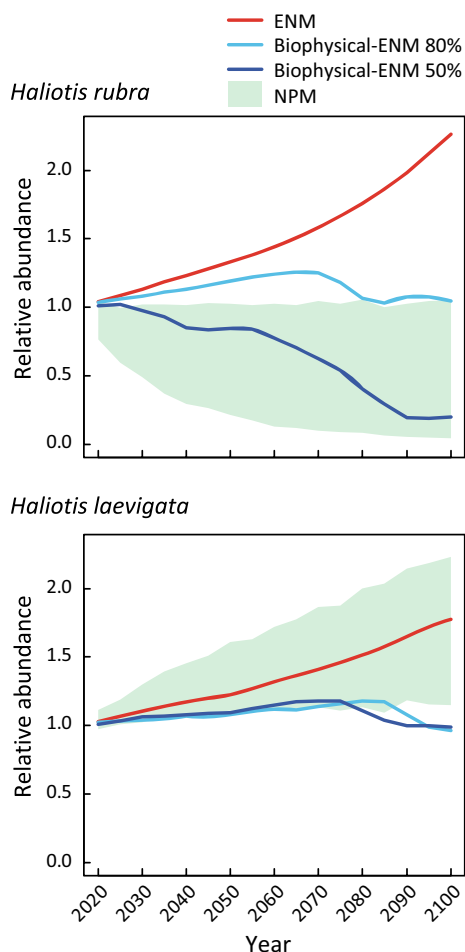
Fig. 5 Uncertainty in forecast change in relative abundance of *Haliotis rubra* and *H. laevigata* for a regionally skilful multi general circulation models averaged forecast and reference greenhouse gas emissions scenario. Modelling approaches are identical to Fig. 4, with the exception that for the niche-population model, uncertainty in estimated change in population size is based on the sensitivity analysis (bounded by 5th and 95th percentiles). See Methods for further detail.

2006); as we show here, this does not necessarily occur. A negative or non-linear relationship between AOO and total population size has similarly been forecast as a response to climate change among some plants and vertebrates (Harris *et al.*, 2012; Fordham *et al.*, 2013a).

In most cases, ENMs are built with the assumption that a species is in equilibrium with its present-day climate, yet dispersal-limitation can constrain a species from accessing all habitable areas (Ehrlén & Eriksson, 2000), and human interference can prevent establishment or modify abundances (Araújo & Peterson, 2012). Accounting for movement in choice of study extent (Barve *et al.*, 2011) and temporal calibration of species' current ranges using the fossil record (Nogués-Bravo, 2009; Maiorano *et al.*, 2013) can improve phenomenological

predictions in such situations. However, neither of these approaches explicitly account for important biotic processes, such as species interactions, which can restrict occupancy in potentially habitable areas (Kissling *et al.*, 2012). Such interactions are relevant in our case study – despite commercial catches of *H. rubra* and *H. laevigata* being approximately stable over the last 40 years (Mayfield *et al.*, 2012), fishing and environmental forcing has strongly influenced local abalone abundance and metapopulation dynamics in some areas (Shepherd & Brown, 1993; Shepherd & Rodda, 2001; Mayfield *et al.*, 2011, 2012). Thus, we expect that recent human exploitation has altered abalone abundance patterns, at least at the spatial scale at which we built our models.

Although we incorporated the seascape variation in exploitation rates as predictors in ENMs (Mellin *et al.*, 2012), the available harvest data were coarse in spatial resolution and could not distinguish exploitation rates for individual reefs. Furthermore, we built ENMs using survey data from South Australia and validated projections using an independent, spatially explicit data set of abalone abundance patterns in Victoria (Mellin *et al.*, 2012). This out-of-sample verification approach provides a rigorous test of model predictive skill (Franklin, 2009) if the combined datasets appropriately characterize the relationship between abundance (or occurrence) and important environmental gradients. Given that March SST is likely to reduce *H. rubra* and *H. laevigata* performance at high temperatures, which was detected by the niche-population models but not the ENMs, we conclude that the distributions were not in equilibrium with the physiologically important March SST gradient because of historical fishing and its interaction with metapopulation processes (i.e. source-sink dynamics and dispersal-limitation).

We expect that March SST will become an important driver of future abundance patterns due to its influence on abalone reproduction (Fordham *et al.*, 2013b). Thus, modelling physiological tolerances as well as selected environmental conditions using biophysical-ENMs and niche-population models should provide better predictions of range movement under climate change. In contrast to ENM forecasts, which suggest a strong positive influence of climate change on the Australian abalone industry, biophysical-ENMs and niche-population models predicted that rapid climate change will (i) reduce the AOO and abundance of *H. rubra* in South Australia, thereby restricting commercial catches; and (ii) reduce the AOO of *H. laevigata*, but not necessarily population size or commercial harvests. Even when uncertainty in the niche-population model is taken into account, ENM estimates of change in population size for *H. rubra* remain notably different to those from the more complex model. However, ENM estimates of

change in population size for *H. laevigata* (the less temperature sensitive species) did not exceed the uncertainty bounds associated with the niche-population model under a 7-model reference greenhouse gas emission scenario. These results, especially for *H. rubra*, provide evidence that physiological information can strengthen estimates of the influence of climate change on species' range and abundance if (i) human-mediated changes in environmental conditions alter a species' spatial abundance patterns; (ii) distribution data do not adequately represent important environmental gradients driving abundance (and occurrence) patterns; and (iii) projections are generated beyond the range of environmental values used to calibrate the correlative model. Likewise, our results suggest that using physiological information to modify ENM predictions (i.e. using biophysical-ENMs), can result in over- or under-estimation of the magnitude of forecast change in AOO and abundance (depending on the biophysical threshold), because unlike niche-population models, metapopulation processes are not considered.

Simple correlative models and more complex coupled models gave similar predictions for the presence or absence of abalone at sites used to calibrate the models (based on cross-validation κ), indicating that uncertainties underlying the ENM and demographic model components of niche-population models are not fully additive. Fully additive model uncertainties would have resulted in the prediction error of the niche-population model being much larger than that of the ENM, because the output from the ENM was used as a nested input for the niche-population model. Niche-population models were more skilful than ENMs and biophysical-ENMs at reproducing occupancy in 2015 for *H. rubra* and *H. laevigata* at independent reef locations based on verification data generated by expert opinion. However, all models incorrectly projected the presence of abalone along the Coorong coast, and in parts of both the Spencer Gulf and Gulf St Vincent, today. This is probably because of a combination of predictor uncertainty (Watts *et al.*, 2011) and regional environmental conditions not reflected in our model parameters – for example, inshore rocky reefs in the Coorong region tend to have small ephemeral abalone populations. Furthermore, the region has undergone major human-induced changes in hydrology (Shuttleworth *et al.*, 2005), a characteristic not captured by our models. Predictor uncertainty could be potentially reduced in future models by incorporating information on the location of soft-sediment trawl fisheries, which are now tracked accurately. This information could strengthen the spatial accuracy of reef habitats and, in turn, predictions of abalone occurrence in the Coorong and areas of the upper Spencer Gulf and Gulf St Vincent (Fig. 1 –

sites that are marked as not unoccupied in 2015). Rapid population growth, as predicted under the PCM reference scenario (Table 1) (driven by high August and low March SST; Fig. S1), and observed across models of varying complexity is also unlikely to occur. This is because the PCM has poor retrospective skill (at least compared to 7-model and CCSM) in reproducing recent global and regional (Indian and Pacific Oceans) SST records (Fordham *et al.*, 2013b), leading to reduced confidence in future projections (Fordham *et al.*, 2011).

An important and additional strength of niche-population models is their ability to be used in 'simulation experiments' that evaluate the efficacy of alternative climate-management options (Fordham *et al.*, 2013a), within an economic optimization framework (Wintle *et al.*, 2011). Because abalone are amenable to introduction and translocation (Dixon *et al.*, 2006), our niche-population model results could be used, in a management context, to guide the translocation of *H. rubra* and *H. laevigata* to future habitats predicted to be climatically suitable and stable (Fordham *et al.*, 2012b), thereby (i) reducing the risk that the velocity of climate change will outpace dispersal rate, and (ii) enhancing resilience and potential sustainability of the abalone fishery. By using a representative set of climate futures in the underpinning forecast, the long-term ecological and economic usefulness of establishing translocation sites and refugia (to replenish stocks in surrounding harvest zones) in regions consistently forecast to experience favourable future SSTs can be tested explicitly.

In conclusion, integrative ecological models that aim to link habitat suitability with biological processes should estimate range shifts under climate change better than simpler models by accounting for important biotic and abiotic processes and their interactions, provided adequate data are available to determine structural relationships and fit the associated parameters (Fordham *et al.*, 2013a). In this marine case study of commercially important yet climatically sensitive abalone stocks, we show the overriding importance of considering metapopulation dynamics, as well as biophysical processes and environmental relationships, when examining the dynamics of ranges through time.

Acknowledgements

References

Akçakaya HR, Root WT (2005) *RAMAS GIS: Linking Landscape Data With Population Viability Analysis (Version 5.0)*. Applied Biomathematics, Setauket, New York.

Akçakaya HR, Butchart SHM, Mace GM, Stuart SN, Hilton-Taylor C (2006) Use and misuse of the IUCN Red List Criteria in projecting climate change impacts on biodiversity. *Global Change Biology*, **12**, 2037–2043.

Anderson BJ, Akçakaya HR, Araujo MB, Fordham DA, Martinez-Meyer E, Thuiller W, Brook BW (2009) Dynamics of range margins for metapopulations under climate change. *Proceedings of the Royal Society of London Series B-Biological Sciences*, **276**, 1415–1420.

Araújo M, Peterson AT (2012) Uses and misuses of bioclimatic envelope modelling. *Ecology*, **93**, 1527–1539.

Austin M (2007) Species distribution models and ecological theory: a critical assessment and some possible new approaches. *Ecological Modelling*, **200**, 1–19.

Austin MP, Van Niel KP (2011) Improving species distribution models for climate change studies: variable selection and scale. *Journal of Biogeography*, **38**, 1–8.

Babcock R, Keesing J (1999) Fertilization biology of the abalone *Haliotis laevigata*: laboratory and field studies. *Canadian Journal of Fisheries and Aquatic Sciences*, **56**, 1668–1678.

Bardos DC, Day RW, Lawson NT, Linacre NA (2006) Dynamical response to fishing varies with compensatory mechanism: an abalone population model. *Ecological Modelling*, **192**, 523–542.

Barve N, Barve V, Jiménez-Valverde A *et al.* (2011) The crucial role of the accessible area in ecological niche modeling and species distribution modeling. *Ecological Modelling*, **222**, 1810–1819.

Buckley LB (2008) Linking traits to energetics and population dynamics to predict lizard ranges in changing environments. *American Naturalist*, **171**, E1–E19.

Buckley LB, Urban MC, Angilletta MJ, Crozier LG, Rissler LJ, Sears MW (2010) Can mechanism inform species' distribution models? *Ecology Letters*, **13**, 1041–1054.

Buckley LB, Waaser SA, Maclean HJ, Fox R (2011) Does including physiology improve species distribution model predictions of responses to recent climate change? *Ecology*, **92**, 2214–2221.

Cheung WWL, Dunne J, Sarmiento JL, Pauly D (2011) Integrating ecophysiology and plankton dynamics into projected maximum fisheries catch potential under climate change in the Northeast Atlantic. *ICES Journal of Marine Science: Journal du Conseil*, **68**, 1008–1018.

Cheung WWL, Sarmiento JL, Dunne J *et al.* (2012) Shrinking of fishes exacerbates impacts of global ocean changes on marine ecosystems. *Nature Climate Change*, **3**, 254–258.

Clark RA, Fox CJ, Viner D, Livermore M (2003) North Sea cod and climate change – modelling the effects of temperature on population dynamics. *Global Change Biology*, **9**, 1669–1680.

Clarke LE, Edmonds JA, Jacoby HD, Pitcher H, Reilly JM, Richels R (2007) *Scenarios of Greenhouse Gas Emissions and Atmospheric Concentrations*. A Report by the Climate Change Science Program and the Subcommittee on Global Change Research. Department of Energy, Office of Biological & Environmental Research. Washington, DC. pp. 1–154.

Cohen J (1960) A Coefficient of Agreement for Nominal Scales. *Educational and Psychological Measurement*, **20**, 37–46.

Collins WD, Bitz CM, Blackmon ML *et al.* (2006) The community climate system model version 3 (CCSM3). *Journal of Climate*, **19**, 2122–2143.

Crozier L, Dwyer G (2006) Combining population-dynamic and ecophysiological models to predict climate-induced insect range shifts. *American Naturalist*, **167**, 853–866.

Dixon CD, Day RW, Huchette SMH, Shepherd SA (2006) Successful seeding of hatchery-produced juvenile greenlip abalone to restore wild stocks. *Fisheries Research*, **78**, 179–185.

Dormann CF, Schymanski SJ, Cabral J *et al.* (2012) Correlation and process in species distribution models: bridging a dichotomy. *Journal of Biogeography*, **39**, 2119–2131.

Dulvy NK, Rogers SI, Jennings S, Stelzenmuller V, Dye SR, Skjoldal HR (2008) Climate change and deepening of the North Sea fish assemblage: a biotic indicator of warming seas. *Journal of Applied Ecology*, **45**, 1029–1039.

Edwards M, Richardson AJ (2004) Impact of climate change on marine pelagic phenology and trophic mismatch. *Nature*, **430**, 881–884.

Ehrlén J, Eriksson O (2000) Dispersal limitation and patch occupancy in forest herbs. *Ecology*, **81**, 1667–1674.

Elith J, Kearney M, Phillips S (2010) The art of modelling range-shifting species. *Methods in Ecology and Evolution*, **1**, 330–342.

Fordham DA, Wigley TML, Brook BW (2011) Multi-model climate projections for biodiversity risk assessment. *Ecological Applications*, **21**, 3317–3331.

Fordham DA, Akçakaya HR, Araújo MB *et al.* (2012a) Plant extinction risk under climate change: are forecast range shifts alone a good indicator of species vulnerability to global warming? *Global Change Biology*, **18**, 1357–1371.

Fordham DA, Watts MJ, Delean S, Brook BW, Heard LMB, Bull CM (2012b) Managed relocation as an adaptation strategy for mitigating climate change threats to the persistence of an endangered lizard. *Global Change Biology*, **18**, 2743–2755.

Fordham DA, Wigley TML, Watts MJ, Brook BW (2012c) Strengthening forecasts of climate change impacts with multi-model ensemble averaged projections using MAGICC/SCENGEN 5.3. *Ecography*, **35**, 4–8.

Fordham DA, Akcakaya HR, Keith DA, Brook BW (2013a) Tools for integrating range change, extinction risk and climate change information into conservation management. *Ecography*, doi:10.1111/j.1600-0587.2013.00147.x

Fordham DA, Brook BW, Caley MJ, Bradshaw CJA, Mellin C (2013b) Conservation management and sustainable harvest quotas are sensitive to choice of climate modelling approach for two marine gastropods. *Diversity and Distributions*, doi: 10.1111/ddi.12092

Franklin J (2009) *Mapping Species Distributions: Spatial Inference and Prediction*. Cambridge University Press, Cambridge.

Gilroy A, Edwards SJ (1998) Optimum temperature for growth of Australian abalone: preferred temperature and critical thermal maximum for blacklip abalone, *Haliotis rubra* (Leach), and greenlip abalone, *Haliotis laevigata* (Leach). *Aquaculture Research*, **29**, 481–485.

Grubert MA, Ritar AJ (2004a) The effect of temperature on the embryonic and larval development of blacklip (*Haliotis rubra*) and greenlip (*H. laevigata*) abalone. *Invertebrate Reproduction & Development*, **45**, 197–203.

Grubert MA, Ritar AJ (2004b) Temperature effects on the dynamics of gonad and oocyte development in captive wild-caught blacklip (*Haliotis rubra*) and greenlip (*H. laevigata*) abalone. *Invertebrate Reproduction & Development*, **45**, 185–196.

Hanski I (1999) *Metapopulation Ecology*. Oxford University Press, Oxford, UK.

Harley CDG, Randall Hughes A, Hultgren KM *et al.* (2006) The impacts of climate change in coastal marine systems. *Ecology Letters*, **9**, 228–241.

Harris JO, Burke CM, Edwards SJ, Johns DR (2005) Effects of oxygen supersaturation and temperature on juvenile greenlip, *Haliotis laevigata* Donovan, and blacklip, *Haliotis rubra* Leach, abalone. *Aquaculture Research*, **36**, 1400–1407.

Harris JBC, Fordham DA, Mooney PA *et al.* (2012) Managing the long-term persistence of a rare cockatoo under climate change. *Journal of Applied Ecology*, **49**, 785–794.

Iman RL, Campbell JE, Helton JC (1981) An approach to sensitivity analysis of computer models. I - Introduction, input, variable selection and preliminary variable assessment. *Journal of Quality Technology*, **13**, 174–183.

Kearney M, Porter W (2009) Mechanistic niche modelling: combining physiological and spatial data to predict species ranges. *Ecology Letters*, **12**, 334–350.

Kearney M, Phillips BL, Tracy CR, Christian KA, Betts G, Porter WP (2008) Modelling species distributions without using species distributions: the cane toad in Australia under current and future climates. *Ecography*, **31**, 423–434.

Kearney MR, Wintle BA, Porter WP (2010) Correlative and mechanistic models of species distribution provide congruent forecasts under climate change. *Conservation Letters*, **3**, 203–213.

Keith DA, Akcakaya HR, Thuiller W *et al.* (2008) Predicting extinction risks under climate change: coupling stochastic population models with dynamic bioclimatic habitat models. *Biology Letters*, **4**, 560–563.

Kissling WD, Dormann CF, Groeneveld J *et al.* (2012) Towards novel approaches to modelling biotic interactions in multispecies assemblages at large spatial extents. *Journal of Biogeography*, **39**, 2163–2178.

Liu C, Berry PM, Dawson TP, Pearson RG (2005) Selecting thresholds of occurrence in the prediction of species distributions. *Ecography*, **28**, 385–393.

Maiorano L, Cheddadi R, Zimmermann NE *et al.* (2013) Building the niche through time: using 13,000 years of data to predict the effects of climate change on three tree species in Europe. *Global Ecology and Biogeography*, **22**, 302–317.

Mayfield S, Chick RC, Carlson IJ, Ward TM (2011) Invertebrate dive fisheries can be sustainable: forty years of production from a greenlip abalone fishery off Southern Australia. *Reviews in Fisheries Science*, **19**, 216–230.

Mayfield S, Mundy C, Gorfine H, Hart AM, Worthington D (2012) Fifty Years of Sustained Production from the Australian Abalone Fisheries. *Reviews in Fisheries Science*, **20**, 220–250.

McShane PE, Smith MG (1989) Direct measurement of fishing mortality in abalone (*Haliotis rubra* Leach) off southeastern Australia. *Fisheries Research*, **8**, 93–102.

McShane PE, Smith MG (1991) Recruitment variation in sympatric populations of *Haliotis rubra* (Mollusca: Gastropoda) in southeast Australian waters. *Marine Ecology Progress Series*, **73**, 203–210.

McShane PE, Black KP, Smith MG (1988) Recruitment processes in *Haliotis rubra* (Mollusca: Gastropoda) and regional hydrodynamics in southeastern Australia imply localized dispersal of larvae. *Journal of Experimental Marine Biology and Ecology*, **124**, 175–203.

Mellin C, Russell BD, Connell SD, Brook BW, Fordham DA (2012) Geographic range determinants of two commercially important marine molluscs. *Diversity and Distributions*, **18**, 133–146.

Miller KJ, Maynard BT, Mundy CN (2009) Genetic diversity and gene flow in collapsed and healthy abalone fisheries. *Molecular Ecology*, **18**, 200–211.

Monahan WB (2009) A mechanistic niche model for measuring species' distributional responses to seasonal temperature gradients. *PLoS ONE*, **4**, e7921.

Nogués-Bravo D (2009) Predicting the past distribution of species climatic niches. *Global Ecology and Biogeography*, **18**, 521–531.

Perry AL, Low PJ, Ellis JR, Reynolds JD (2005) Climate change and distribution shifts in marine fishes. *Science*, **308**, 1912–1915.

Peterson AT, Soberón J, Pearson RG, Anderson RP, Nakamura M, Martinez-Meyer E, Araújo MB (2011) *Ecological Niches and Geographical Distributions*. Princeton University Press, New Jersey.

Plagányi É, Butterworth D, Burgener M (2011) Illegal and unreported fishing on abalone—Quantifying the extent using a fully integrated assessment model. *Fisheries Research*, **107**, 221–232.

Pörtner H-O (2010) Oxygen- and capacity-limitation of thermal tolerance: a matrix for integrating climate-related stressor effects in marine ecosystems. *The Journal of Experimental Biology*, **213**, 881–893.

Russell BR, Connell SD, Mellin C, Brook BW, Burnell OW, Fordham DA (2012) Predicting the distribution of commercially viable invertebrate stocks under future climate. *PLoS ONE*, **7**, e46554.

Shepherd SA (1990) Studies on Southern Australian Abalone (Genus *Haliotis*). XII. Long-term recruitment and mortality dynamics of an unfished population. *Marine and Freshwater Research*, **41**, 475–492.

Shepherd SA (1998) Studies on southern Australian abalone (genus *Haliotis*) - XIX: long-term juvenile mortality dynamics. *Journal of Shellfish Research*, **17**, 813–825.

Shepherd SA, Breen PA (1992) Mortality in abalone: its estimation, variability and causes. In: *Abalone of the World: Biology, Fisheries and Culture* (eds Shepherd SA, Tegner MJ, Guzman Del Proo SA), pp. 276–304. Fishing News Books, London.

Shepherd SA, Brown LD (1993) What is an abalone stock: implications for the role of refugia in conservation. *Canadian Journal of Fisheries and Aquatic Sciences*, **50**, 2001–2009.

Shepherd SA, Partington D (1995) Studies on southern Australian abalone (Genus *Haliotis*), 16. Recruitment, habitat and stock relations. *Marine and Freshwater Research*, **46**, 669–680.

Shepherd SA, Rodda KR (2001) Sustainability demands vigilance: evidence for serial decline of the greenlip abalone fishery and a review of management. *Journal of Shellfish Research*, **20**, 829–841.

Shuttleworth B, Woidt A, Paparella T, Herbig S, Walker D (2005) The dynamic behaviour of a river-dominated tidal inlet, River Murray, Australia. *Estuarine, Coastal and Shelf Science*, **64**, 645–657.

Stanton JC, Pearson RG, Horning N, Ersts P, Reşit Akçakaya H (2012) Combining static and dynamic variables in species distribution models under climate change. *Methods in Ecology and Evolution*, **3**, 349–357.

Sumaila UR, Cheung WWL, Lam VWY, Pauly D, Herrick S (2011) Climate change impacts on the biophysics and economics of world fisheries. *Nature Climate Change*, **1**, 449–456.

Washington WM, Weatherly JW, Meehl GA *et al.* (2000) Parallel climate model (PCM) control and transient simulations. *Climate Dynamics*, **16**, 755–774.

Watson JR, Siegel DA, Kendall BE, Mitarai S, Rassweiller A, Gaines SD (2011) Identifying critical regions in small-world marine metapopulations. *Proceedings of the National Academy of Sciences*, **108**, E907–E913.

Watts MJ, Li Y, Russell BD, Mellin C, Connell SD, Fordham DA (2011) A novel method for mapping reefs and subtidal rocky habitats using artificial neural networks. *Ecological Modelling*, **222**, 2606–2614.

Webster MA, Petkovic P (2005) *Australian Bathymetry and Topography Grid*. Geoscience Australia, Canberra.

Wigley TML, Clarke LE, Edmonds JA *et al.* (2009) Uncertainties in climate stabilization. *Climatic Change*, **97**, 85–121.

Wintle BA, Bekessy SA, Keith DA *et al.* (2011) Ecological-economic optimization of biodiversity conservation under climate change. *Nature Climate Change*, **1**, 355–359.

Supporting Information

Additional Supporting Information may be found in the online version of this article:

Appendix S1. Extended description of methods.

Figure S1. Forecast average March and August sea-surface temperatures.

Figure S2–3. Forecast change in spatial abundance between 2015 and 2100 for *Haliotis rubra* and *Haliotis laevigata* according to the CCSM-3.

Figure S4–5. Forecast change in spatial abundance between 2015 and 2100 for *Haliotis rubra* and *Haliotis laevigata* based on the PCM.

Figure S6. Forecast change in relative abundance of *Haliotis rubra* and *Haliotis laevigata* based on the CCSM-3.

Figure S7. Harvest catch for *Haliotis rubra* and *Haliotis laevigata*.